

Modeling Visual Cortical Contrast Adaptation Effects

E.V. Todorov¹, A.G. Siapas¹, D. C. Somers¹, and S. B. Nelson²

¹Department of Brain and Cognitive Sciences, MIT, Cambridge, MA 02139

²Department of Biology, Brandeis University, Waltham, MA 02154

emo@ai.mit.edu, thanos@ai.mit.edu, somers@ai.mit.edu, nelson@binah.cc.brandeis.edu

Abstract

We demonstrate a detailed visual cortical circuit which exhibits robust contrast adaptation properties, consistent with physiological observations in V1. The adaptation mechanism we employ is activity-dependent synaptic depression at thalamocortical and local intra-cortical synapses. Model contrast response functions (CRF) shift so that cells remain maximally responsive to changes around the recent average stimulus contrast level. Hysteresis effects for both stimulus contrast and orientation are achieved; orientation hysteresis is weaker, and depends exclusively on intracortical adaptation. Following stimulation of the receptive field (RF) surround, RFs dynamically expand to “fill in” for the missing stimulation in the RF center; in our model this expansion results from adaptation of local inhibitory synapses, triggered by excitation from long range horizontal projections. All adaptation effects are achieved using the same synaptic depression mechanism at both thalamocortical and intracortical synapses.

Introduction

Nearly all neurons in the primary visual cortex (V1) exhibit reduced responsiveness after exposure to high contrast stimuli [1, 3, 8, 10, 13]. This contrast adaptation appears to have functional utility as a cortical gain control mechanism: a neuron’s contrast response function rapidly shifts so that the neuron remains maximally responsive to both contrast increments and decrements around the recent mean contrast level [13]. Adaptation effects occur rapidly and can be observed after even a single, brief (50 msec) stimulus presentation [3]. Recovery from adaptation occurs more slowly and hysteresis effects are readily observable in contrast response functions [3, 11]. Adaptation effects also depend on stimulus properties other than contrast, such as orientation. Given a fixed contrast level, hysteresis effects occur in the orientation domain; however, orientation hysteresis effects are smaller than contrast hysteresis effects for the same firing levels, indicating that different mechanisms may underlie the two effects [3].

The mechanisms underlying contrast adaptation, despite intense study, remain unclear. This phenomenon almost certainly arises within cortex since it exhibits inter-ocular transfer [8, 15] and since lateral geniculate (LGN) neurons lack contrast adaptation [3, 10, 13]. The hypothesis that “fatigue” of cortical neurons leads to adaptation [2] can be excluded since pharmacological induction of firing by glutamate iontophoresis does not induce adaptation in a cell and similarly blockade of the cell’s response with GABA does not abolish adaptation effects [18]. Rather, adaptation may be a network effect since adaptation effects depend primarily on the mean stimulus contrast level over a recent time window. Several authors [3, 7, 13] have suggested that contrast adaptation effects may be accounted for by an inhibitory process, possibly involving divisive normalization. However, inhibitory mechanisms have not found experimental support. Blockade of GABA-mediated inhibition does not disrupt adaptation [3, 5] and the suggestion that divisive normalization is achieved via shunting inhibition is inconsistent with intracellular recordings in visual cortex [6]. Here, we

explore a different hypothesis, that short-term changes in synaptic transmission properties at thalamocortical and intracortical synapses can account for cortical adaptation effects. Specifically, we explore synaptic changes that depend on pre-synaptic activity only. These explorations are carried out within a detailed cortical circuit structure which we have previously used to explain experimental data on orientation selectivity [16].

Short-term adaptation effects following stimulation of the RF surround have also been observed [14, 4]. Prolonged exposure to an “artificial scotoma” stimulus that covers an area outside a large central blank region causes increased responsiveness in cells whose RFs lie well within the blank region. Testing with minimal bar stimulation also reveals a substantial expansion of the classical RF [14]. Reverse correlation analysis of white noise stimulation indicates that normally subthreshold RF regions become suprathreshold, but suggests that the effects are better characterized as a uniform gain increase than as an RF expansion [4]. It has been suggested that this phenomenon is due to changes in the input from long-range horizontal projections [14]. Since most of the expansion is localized to the scotoma region, we think that a more likely candidate mechanism is a change in the local circuit gain, triggered by inputs from horizontal projections. We demonstrate that synaptic depression mechanisms which achieve normal contrast adaptation can also produce local circuit gain changes consistent with the artificial scotoma results.

Methods

Computer simulations were performed on model circuits composed of interacting excitatory and inhibitory cortical neurons which received feedforward excitation from LGN neurons. Peak conductances at thalamocortical excitatory, intracortical excitatory, and intracortical inhibitory synapses varied approximately inversely with the recent average firing rates of the pre-synaptic neurons. Cortical neurons were implemented as “improved integrate-and-fire” neurons [19] with membrane time constant and resistance values chosen to match values found experimentally for fast-spiking (inhibitory) and regular-spiking (excitatory) neurons [9]. Conductance changes (for a single spike event) were modeled as α -functions, and parameter values were similar to those used in [16]. In all cases the probability of a synaptic connection between two V1 neurons was 0.1. LGN responses increased linearly with log contrast (up to 50Hz at max contrast) and individual responses were described by Poisson processes. LGN neurons provided feedforward inputs to both excitatory and inhibitory cortical neurons (10 LGN cells to a V1 cell).

Synaptic adaptation was modeled as a reduction of post-synaptic conductance (and thus PSP size), dependent upon pre-synaptic firing (as observed in [12]). Each synapse had a synaptic efficacy, w , and an adaptation level, $AD(t)$, associated with it. If the pre-synaptic cell generated an action potential at time t , the peak of the conductance change in the post-synaptic cell was $w(1 - AD(t))$. The adaptation level increased after each spike according to $AD(t) = AD(t) + (AD_{max} - AD(t))AD_{inc}$ and passively decayed with time constant τ : $AD(t + 1) = AD(t)e^{-1/\tau}$. The constants AD_{max} and AD_{inc} corresponded to the maximum adaptation level ($AD_{max} < 1$) and to the percent increase for each spike, respectively. This mechanism is consistent with two possible physiological phenomena: i) for each action potential the synapse releases a unit volume of some substance, which acts to increase the local concentration of that substance; AD_{max} is the maximum concentration level that can be achieved before diffusion or uptake mechanisms balance the unitary increase completely; ii) the adaptation level is increased by a constant amount for each vesicle release, but release probability decreases with adaptation. Although we modeled adaptation as decreasing PSP size, it is possible (and mathematically consistent with our model) that it actually

corresponds to a decrease in release probability for synapses with multiple release sites. Note that for a fixed firing rate M of the pre-synaptic cell over a sufficiently long period of time, $AD(t)$ will asymptote to $A(M)$ satisfying the equation $(AD_{max} - A(M))AD_{inc}M = A(M)(1 - e^{-1/\tau})$, or $A(M) = AD_{max}M / (AD_{inc}M + 1 - e^{-1/\tau})$, which is an upward convex function of M .

Due to the computational load of time-varying synapses, the size of the cortical circuits was restricted to include only the cortical dimensions needed to explore the data set at hand. As a result, three different circuits were employed. The first model (CRFs, Gain Control) was a homogeneous population of 200 excitatory and 50 inhibitory neurons, corresponding to a small population in V1 cells with similar RF position and orientation tuning. The second model (Hysteresis) consisted of 1000 excitatory and 250 inhibitory neurons, with overlapping RFs, and orientation tuning ranging from 0 to 180 degrees. In the hysteresis model, the total LGN input to each cortical neuron exhibited a modest orientation bias that was sharpened by intracortical connections (see [16]). Cortical neurons were organized into orientation columns and received substantial input from both cortical inhibitory and cortical excitatory neurons. Both sets of inputs came most densely from the same or nearby orientation columns with the inhibition from a somewhat broader set of orientations. The third model (artificial scotoma) represented visual space rather than orientation. The only change in connectivity was the addition of long-range horizontal excitatory projections, that contacted equally both excitatory and inhibitory cells.

Stimuli were chosen to represent the average effects of moving, oriented sine-wave gratings. In order to reduce computational times, LGN neuronal firing rates were held at constant contrast-dependent level for the course of a simulation. It is assumed that moving gratings stimulate all LGN cells equally, resulting in a constant adaptation level for thalamocortical synapses when contrast is held fixed and only orientation is varied. Adaptation and recovery effects occurred at both thalamocortical and intracortical synapses. Stimuli were presented 10 times each and spike totals were used to generate contrast response functions. The CRFs for the excitatory population are presented. For contrast hysteresis studies, optimally oriented stimuli were presented first in order of increasing contrast and then in order of decreasing contrast, one presentation in each direction for 10 loops. Similarly, in the orientation hysteresis studies, high contrast stimuli were presented, rotating from non-preferred to preferred and then back.

Results

Before we can approach the phenomenon of contrast adaptation, we need a detailed model that produces plausible (i.e. saturating) contrast response functions without adaptation. (Note that the response of an isolated neuron to injected current saturates only at unphysiologically high firing rates). We have recently developed such a model [17] which we briefly describe here. LGN input is biased towards the excitatory (rather than inhibitory) cortical cells, and as a result they (on the average) respond at lower contrast levels. Thus, the steeply increasing portion of the response function is dominated by recurrent self-excitation. Saturation results from a balance between excitation and inhibition, once the inhibitory population enters the linear range of its response.

We now consider how the response of this recurrent system changes when different groups of synapses are modified. Figure 1 summarizes the effects of separately modifying thalamocortical (A), cortical excitatory (B), cortical inhibitory (C), and all cortical (D) synapses, by +/- 10%. In each panel, the arrow marks the direction of decreasing synaptic

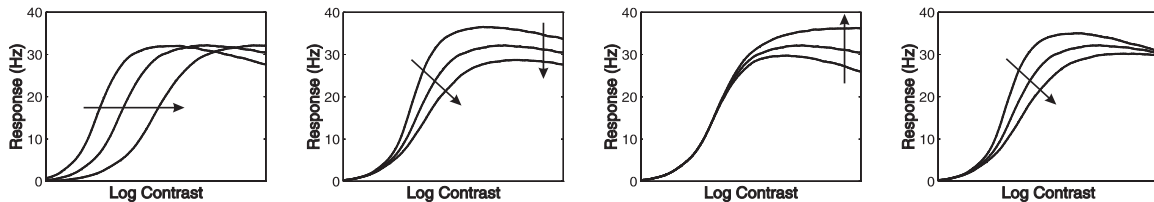


Figure 1: Synaptic depression shifts CRFs.

strength, and the curve in the middle is the same (non-adapted) CRF. Decreasing the efficacy of thalamocortical synapses (A) results in an almost pure rightward shift of the CRF. This pure rightward shift is also achieved in a model of Heeger [7] by increasing the size of a divisive inhibitory term. Our mechanism has the advantages that: i) it is independent of cortical inhibitory signaling and thus is compatible with inhibitory blockade studies; and ii) since LGN neurons themselves do not adapt to contrast, an invariant measure of stimulus contrast is always available at the site of adaptation. Decreasing the strength of intracortical excitation (B) has two effects: i) the slope of the steep part of the CRF decreases, since it is determined by the strength of recurrent self-excitation; ii) saturation occurs at a lower level, since it is the outcome of a balance between recurrent excitation and inhibition. Decreasing intracortical inhibition (C) mostly affects the saturating part of the CRF - there is less saturation, and it occurs at a higher level (the steep part of the CRF may also be affected if extra inhibitory subpopulations are added). If we now modify simultaneously both intracortical excitatory and inhibitory synapses (D), the effects on the saturating part of the CRF from (B) and (C) essentially cancel each other, and the only effect left is the change of slope in the steep part of the CRF. Thus, adaptation at thalamocortical synapses shifts the CRF horizontally, while adaptation at intracortical synapses modifies the slope of the steep part of the CRF. For different synaptic efficacies in the recurrent circuit, depression at intracortical synapses can also result in upward and downward shifts of the CRF. Adaptation at intracortical excitatory synapses can also yield rightward CRF shifts, provided that spontaneous cortical excitation contributes to “resting” responses.

Combination of these adaptation mechanisms into a single model yields robust contrast gain control. We use Model 1, with adaptation parameters (AD_{max}, AD_{inc}, τ) the same for all synapses in the model, to simulate the experiment of [13]. For each of 5 contrast levels (uniformly spaced along the log contrast axis), we present the corresponding contrast until adaptation at all synapses asymptotes. The asymptotic cortical responses are shown by the thick CRF in Figure 2. After presenting each of the 5 contrasts, we “freeze” all synapses, and measure the responses to 7 contrast levels, centered around the adaptation contrast level (thin CRFs). In agreement with the reports in [13], for a range of contrast adaptation levels the CRF shifts so as to center the steepest part of the curve at or near that contrast level. This permits the circuit to be very sensitive to contrast increments or decrements around the recent median contrast level. Rightward (and leftward) shifts of the CRF due to thalamocortical synaptic changes are most prominent in this contrast gain control. Upward or downward shifts of the curves are also observed [1]. In our model these shifts result from adaptation at intracortical synapses. We have found that the same adaptation mechanism can produce either upward or downward shifts, depending on the set of synaptic strengths in the cortical population. For higher contrasts, the adapted CRFs have lower slopes, which is a result of the adaptation of cortical excitatory synapses (see Fig 1b). Note the high slopes of the adapted CRFs, which are consistent with a self-excitation loop amplifying thalamic inputs above some threshold.

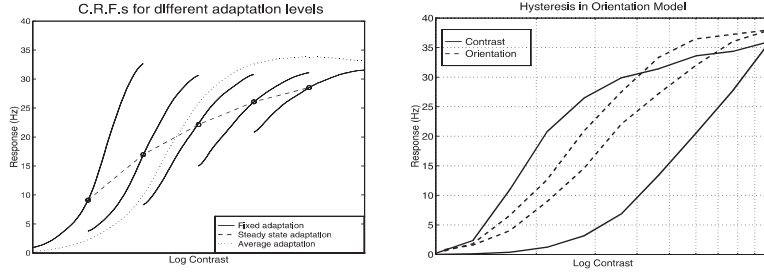


Figure 2: Contrast Gain Control and Hysteresis.

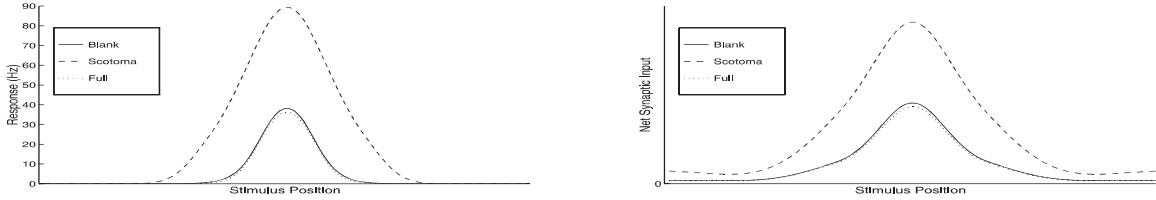


Figure 3: “Artificial Scotoma” Results.

Stimulus presentation order has also been used to isolate adaptation mechanisms [3]. Presentation of optimal orientation stimuli in order from lowest contrast to highest contrast and back yields hysteresis effects, provided that a full cycle can be performed rapidly [3]. This experiment is simulated using Model 2, which includes orientation tuning. Our model 2 achieves this effect (see fig 3) with higher responses exhibited for the march to higher contrasts. This hysteresis results because the level of average recent contrast, as encoded in synapses, is higher on the way down (and thus synaptic efficacy is lower) than on the way up. Another reason is that the “adapted” CRF is centered at the current contrast level (as in figure 2), and even a small step up or down in contrast has a big effect. Contrast hysteresis effects reflect efficacy changes at all synapses. Orientation hysteresis effects have also been observed [3]. Presentation of a high contrast stimulus that shifts from non-preferred orientations to the optimal orientation and then back exhibits higher responses on the way to the optimal response than on the return (see fig 3). This effect is weaker than contrast hysteresis, even for identical levels of firing [3]. In our model, this difference in hysteresis effects reflects a difference in affected mechanisms. With orientation hysteresis, thalamocortical synapses adapt uniformly regardless of the stimulus orientation and thus all hysteresis effects result from selective adaptation of cortical synapses. Because our model cortical cells receive excitation most strongly from like tuned neurons and inhibition from a broader distribution of orientation, when the recent stimulus history is biased toward non-preferred orientations (on the way to preferred) a greater proportion of inhibitory than intracortical excitatory synapses is adapted and thus responses are higher. The converse is true on the way down.

Simulation results for the artificial scotoma stimulus are presented in figures 4a and 4b respectively - the receptive field measured by neuronal firing expanded, and the response in the center increased (4a), while the receptive field measured intra-cellularly (to reveal sub-threshold responses) scaled up (4b). During presentation of the artificial scotoma stimulus, excitation from long-range horizontal projections weakly activated cells in the RF center. Since horizontal projections were not biased, and inhibitory cells are easier to activate, the resulting firing rates were 1 Hz for excitatory, and 5 Hz for inhibitory cells. (Results are consistent with our long-range model [17] in this volume). This small difference was greatly

amplified by the synaptic depression mechanism, which is very sensitive to differences at low firing rates - local excitatory synapses were depressed by about 5%, and local inhibitory synapses by 25%. The difference in depression levels disrupted the balance between excitation and inhibition in the central region of the model, resulting in more net synaptic input (4b) which leads to wider classical receptive fields (4a) due to the thresholding of the neuronal firing mechanism. Note that adaptation to a full field stimulus does not have the same effect, since direct LGN stimulation activates both excitatory and inhibitory cells, which results in balanced depression at intracortical excitatory and inhibitory synapses.

Conclusions

In summary, we proposed a model of the local neuronal circuitry in V1, that relies on a bias of thalamocortical projections towards excitatory cortical neurons to achieve contrast saturation. Our model achieves many fundamental effects of contrast adaptation by utilizing pre-synaptic activity-dependent depression of synaptic efficacy. Such depression effects have been recently observed in V1, and have been implied in contrast adaptation. This explanation has the advantage that it is “parsimonious” while also being consistent with data that indicate multiple mechanisms of contrast adaptation (e.g., contrast and orientation hysteresis), operating at multiple sites. Indeed stimulus adaptation effects are ubiquitous within sensory cortices; synaptic depression appears to be a well-suited candidate for addressing these broader phenomena.

References

- [1] D.G. Albrecht, S.B. Farrar, & D.B. Hamilton (1984) *J. Physiol.* 347: 713-739.
- [2] C. Blakemore, R.H.S. Carpenter, & M. Georgeson (1970). *Nature* 228: 37-39.
- [3] A.B. Bonds (1991) *Vis. Neurosci.* 6: 239-255.
- [4] G.C. DeAngelis, A. Anzai, I. Ohzawa, & R.D. Freeman (1995). *Proc. Natl. Acad. Sci (USA)* 92: 9682-9686.
- [5] E.J. DeBruyn & A.B. Bonds (1986). *Brain Research.* 383: 339-342.
- [6] R.J. Douglas, K.A.C. Martin, & D. Whitteridge (1988). *Nature* 332: 642-644.
- [7] D.J. Heeger (1992). *Vis. Neurosci.* 9: 181-197.
- [8] L. Maffei, A. Fiorentini, & S. Bisti (1973). *Science.* 182: 1036-1038.
- [9] D.A. McCormick, B.W. Connors, J.W. Lighthall, and D.A. Prince, D.A. (1985). *J. Neurophysiol.*, 54: 782.
- [10] J.A. Movshon & P. Lennie (1979). *Nature* 278: 850-852.
- [11] S.B. Nelson (1991). *J. Neurosci.* 11: 344-56.
- [12] S.B. Nelson, J.A. Varela, K. Sen, & L.F. Abbott (1996). *CNS96 Proceedings*, Submitted.
- [13] I. Ohzawa, G. Sclar, & R.D. Freeman (1985). *J. Neurophysiol.* 54: 651-667.
- [14] M.W. Pettet & C.D. Gilbert (1992). *Proc. Natl. Acad. Sci (USA)* 89:8366-8370.
- [15] G. Sclar, I. Ohzawa, & R.D. Freeman (1985). *J. Neurophysiol.* 54: 666-673.
- [16] D.C. Somers, S.B. Nelson, & M. Sur (1995) *J. Neurosci.* 15: 5448-5465.
- [17] D.C. Somers, E.V. Todorov, A.G. Siapas, & M. Sur (1996) *CNS96 Proceedings*, this volume.
- [18] T.R. Vidyasagar (1990). *Neuroscience* 36: 175-179.
- [19] Worgotter, F. & Koch, C. (1991). *J. Neurosci.* 11:1959.